XIII
Hadron spectroscopy

Studies of hadron masses, and of both strong and electromagnetic decays of hadrons, provide insights regarding QCD dynamics over a variety of distance scales. Among various possible theoretical approaches, the potential model has most heavily been employed in this area. We shall start our discussion by considering heavy-quark bound states, which begin to approximate truly nonrelativistic systems and for which the potential model is expected to provide a suitable basis for discussion.

XIII-1 The charmonium and bottomonium systems

Quarkonium is the bound state of a heavy quark Q with its antiparticle. Two such systems, charmonium ($c\bar{c}$) and bottomonium ($b\bar{b}$) have been the subject of much experimental and theoretical study. Due to weak decay of the top quark, the (as yet undiscovered) $t\bar{t}$ system will almost certainly have rather different properties from these, and thus constitutes a special case (*cf.* Sect. XIV–2).

Table XIII–1. Nomenclature for S-wave and P-wave states in the $c\bar{c}$ and $b\bar{b}$ systems.

L	S	Charmonium	Bottomonium
0	1	$\psi(nS)^a$	$\Upsilon(nS)$
	0	$\eta_c(nS)$	$\eta_b(nS)$
1	1	$\chi_{cJ}(nP)$	$\chi_{bJ}(nP)$
	0	$h_c(nP)$	$h_b(nP)$

[a] For historical reasons, the spin-one charmonium ground state is called J/ψ.

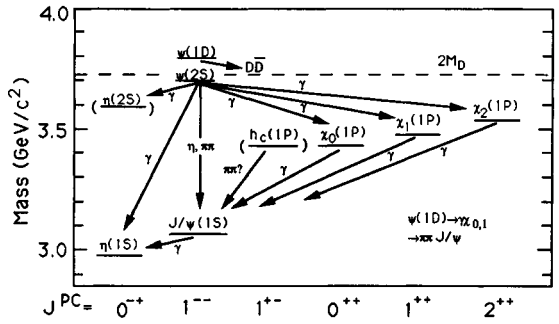

Fig. XIII–1 The low-lying spectrum of charmonium.

Since the quarkonium systems are quark-antiquark composites, we shall employ the set of quantum numbers n, L, S, J introduced in Sect. XI–2. One generally refers to the individual quarkonium levels with the nomenclature of Table XIII–1, although the nL identification is sometimes replaced by either the degree of excitation or the mass, *e.g.* $\psi(2S)$ is called ψ' or $\psi(3686)$. The $n^{2S+1}L_J$ spectroscopic notation is also invoked on occasion.

Figs. XIII–1,2 give a summary of the lightest observed $c\bar{c}$ and $b\bar{b}$ states. At present, there are no firm candidates for $^1P_1$ states in either system and only one reasonably firm D-wave assignment, $\psi(3770)$. The greatest observed degrees of excitation come from the $\psi(nS)$ and $\Upsilon(nS)$ radial towers, reaching up to $n = 6$ for the Υ system. Excitation energies are relatively small on the scale of the bottomonium reduced mass $\mu_b \simeq 2.5$ GeV, but not that of charmonium $\mu_c \simeq 0.8$ GeV. By far, the greater part of the theoretical effort on interpreting quarkonium systems has been performed in the context of nonrelativistic quantum mechanics [QuR 79].

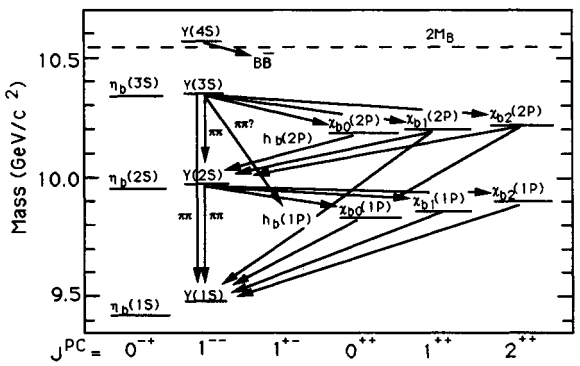

Fig. XIII–2 The low-lying spectrum of bottomonium

Thus, quarkonium mass values are expressed as

$$m_{[nLSJ]} = 2M_Q + E_{[nLSJ]} \quad , \tag{1.1}$$

where $E_{[nLSJ]}$ is obtained by solving the Schrodinger equation for a particle of reduced mass $\mu_Q = M_Q/2$ moving in the field of an assumed potential energy function. In the following, we shall consider several aspects of quarkonium systems.

Lattice studies: The ultimate aim of lattice-gauge studies is to show that the potential picture is a consequence of QCD, and to even specify the quark-antiquark potential itself. Although this program is far from completion, results of lattice simulations are consistent with parameterizing the long-range part of the static $Q\bar{Q}$ potential in pure (*i.e.* without light dynamic quarks) $SU(3)$ gauge theory as [Has 87, Fu 87]

$$V(r) = br - \frac{a}{r} + V_0 \quad , \tag{1.2}$$

where a, b, V_0 are constants and the color dependence between quark and antiquark is that in Eq. (XI–2.4). As noted in Sect. XI–2, the linear 'br' term models a color-flux tube of constant energy density. The coefficient b is commonly described in the lattice-gauge literature as the *string tension*, in reference to the string model of hadrons, and its value is estimated from a string model relation involving the typical slope α' of a hadronic Regge trajectory (*cf.* Table XIII–3),

$$b = (2\pi\alpha')^{-1} \simeq 0.18 \text{ GeV}^2 \quad . \tag{1.3}$$

This is equivalent to a restoring force of about 16 tons!

Numerical studies imply a relation between the string tension b and the confinement scale $\Lambda_{\overline{MS}}$ of QCD [Fu 87],

$$\Lambda_{\overline{MS}} = (0.318 \pm 0.058)\sqrt{b} \simeq 0.13 \pm 0.02 \text{ GeV} \quad . \tag{1.4}$$

If one goes beyond pure gauge theory by including the effects of a light dynamic quark q, the long-range potential between $Q\bar{Q}$ becomes a short-range interaction between $Q\bar{q}$ and $\bar{Q}q$ [Ze 88]. That is, the original interaction between the color charge carried by a heavy quark-antiquark pair becomes screened by the creation of a light quark-antiquark pair in the color field.

Phenomenological potentials: The spectra of quarkonium states already hints at the radial dependence of the $Q\bar{Q}$ potential, with the progression in nL levels suggesting an interaction which lies 'between' coulomb and harmonic oscillator potentials, as depicted in Fig. XIII–3. In practice,

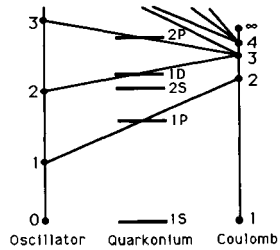

Fig. XIII–3 Energy levels of various potential functions

phenomenological studies of quarkonium are carried out by adopting an *assumed* potential energy function in accord with this behavior, *e.g.**

$$V(r) = \begin{cases} -\dfrac{64\pi^2}{27}\mathcal{F}\left\{\left[q^2 \ln\left(1+(q^2/\Lambda^2)\right)\right]^{-1}\right\} & \{\Lambda \simeq 0.4 \text{ GeV}\}\ , \\ br - a/r & \left\{\begin{matrix} b \simeq 0.18 \text{ GeV}^2 \\ a \simeq 0.52 \end{matrix}\right\}\ , \\ cr^d & \left\{\begin{matrix} c \simeq 6.87 \text{ GeV} \\ d \simeq 0.1 \end{matrix}\right\}\ , \end{cases} \tag{1.5}$$

where $\mathcal{F}\{\ldots\}$ denotes a Fourier transform. The first two of the potentials in Eq. (1.5) are commonly called the 'Richardson' [Ri 79] and 'Cornell' [EiGKLY 80] potentials respectively. They are constructed to mimic QCD by exhibiting a linear confining potential at long distances and single gluon exchange at short distances. The Richardson potential even incorporates the asymptotic freedom property for the strong interaction coupling. The third is a power law potential [Ma 81] which, although not motivated by QCD, can be of use in analytical work or in obtaining simple scaling laws. The power law potential also serves as a reminder of how alternative forms can achieve a reasonable success in fitting $b\bar{b}$ and $c\bar{c}$ spectra, which after all, are primarily sensitive to the limited length scale $0.25 \leq r(\text{fm}) \leq 1$.

From the viewpoint of phenomenology, it is ultimately more useful to appreciate the general features of the $Q\bar{Q}$ static potential than to dwell on the relative virtues and shortcomings of individual models. In this regard, a study of spin dependence is instructive.

Spin dependence: In order to analyze spin-dependent effects in quarkonium without detailed *a priori* knowledge of the interquark potential, we assume an interaction suggested by the QED interaction of Eq. (V–1.16)

* The second and third potentials provide fits only up to an additive constant.

but allowing for a more general vertex structure [Ja 76],

$$V_{\text{general}} = \Gamma_i \tilde{V}_i(q^2) \Gamma_i \ , \qquad (\Gamma = 1, \gamma^\mu, \gamma_5, \gamma^\mu\gamma_5, \sigma^{\mu\nu}) \ , \tag{1.6}$$

where $\tilde{V}_i(q^2)$ represents the propagator of an exchanged quantum. The nonrelativistic limit of this expression, expanded in inverse powers of the heavy-quark masses [EiF 81], yields a sum of static and spin-dependent contributions,

$$V_{\text{general}} = V_0 + V_{\text{spin}} = V_0 + V_{\text{s-o}} + V_{\text{ten}} + V_{\text{s-s}} \ . \tag{1.7a}$$

The potential V_{spin} is seen to generally contain spin-orbit ($V_{\text{s-o}}$), tensor (V_{ten}), and spin-spin ($V_{\text{s-s}}$) components,

$$\begin{aligned} V_{\text{s-o}} &= \left[\frac{\mathbf{s}_Q \cdot \mathbf{r} \times \mathbf{p}_Q}{2M_Q^2} - \frac{\mathbf{s}_{\bar{Q}} \cdot \mathbf{r} \times \mathbf{p}_{\bar{Q}}}{2M_{\bar{Q}}^2} \right] \left[\frac{V_0'}{r} + 2\frac{V_1'}{r} \right] \\ &\quad + \frac{\mathbf{s}_{\bar{Q}} \cdot \mathbf{r} \times \mathbf{p}_Q - \mathbf{s}_Q \cdot \mathbf{r} \times \mathbf{p}_{\bar{Q}}}{M_Q M_{\bar{Q}}} \frac{V_2'}{r} \ , \\ V_{\text{ten}} &= \frac{s_{\text{ten}}}{3M_Q M_{\bar{Q}}} V_3 \qquad [s_{\text{ten}} \equiv 3(\mathbf{s}_Q \cdot \hat{\mathbf{r}})(\mathbf{s}_{\bar{Q}} \cdot \hat{\mathbf{r}}) - \mathbf{s}_Q \cdot \mathbf{s}_{\bar{Q}}] \ , \\ V_{\text{s-s}} &= \frac{\mathbf{s}_Q \cdot \mathbf{s}_{\bar{Q}}}{3M_Q M_{\bar{Q}}} V_4 \ , \end{aligned} \tag{1.7b}$$

where $\mathbf{r} \equiv \mathbf{r}_Q - \mathbf{r}_{\bar{Q}}$. The quantity V_{spin} is expressed in terms of V_0, its radial derivative V_0', and additional contributions $V_i(r), V_i'(r)$ $(i = 1, \ldots, 4)$. Referring to Table XIII–2, we see that the QED Breit-Fermi potential represents a special case, with all nonzero contributions expressed in terms of the static coulomb potential. Also appearing in Table XIII–2 are general forms for vector and scalar vertices. The less interesting pseudoscalar vertex (which does not lead to a static potential) and the axial-vector and tensor vertices (which have only a leading spin-spin interaction) are not included.

Let us apply Eqs. (1.7a,b) to quarkonium by working in the $Q\bar{Q}$ center-of-mass frame with equal constituent quark masses $M_Q = M_{\bar{Q}} \equiv M$. The

Table XIII–2. Spin-dependent potentials.

Interaction	Γ	V_0	V_1	V_2	V_3	V_4
QED	γ^μ	$-\alpha/r$	0	$-\alpha/r$	$3\alpha/r^3$	$8\pi\alpha\delta^{(3)}(\mathbf{r})$
Vector	γ^μ	V_V	0	V_V	$V_V'/r - V_V''$	$2\,\boldsymbol{\nabla}^2 V_V$
Scalar	1	V_S	$-V_S$	0	0	0

spin-dependent potential of Eq. (1.7b) then simplifies to

$$V_{\rm spin} = \frac{1}{2M^2 r}[3V_V' - V_S']\ \mathbf{L}\cdot\mathbf{S} + \frac{1}{6M^2}\left[\frac{V_V'}{r} - V_V''\right] 2S_{\rm ten} + \frac{2}{3M^2}[\boldsymbol{\nabla}^2 V_V]\ \mathbf{s}_Q\cdot\mathbf{s}_{\bar{Q}} \ . \tag{1.8}$$

For the purpose of obtaining mass-splitting relations, we require the computation of various expectation values in the basis of $\Psi_{[LSJ]}$ states,

$$\langle \mathbf{L}\cdot\mathbf{S}\rangle = \frac{\langle \mathbf{J}^2\rangle - 4}{2} = \begin{cases} 1 & (^3P_2)\ , \\ -1 & (^3P_1)\ , \\ -2 & (^3P_0)\ , \end{cases}$$

$$\langle 2S_{\rm ten}\rangle = -\frac{12\langle \mathbf{L}\cdot\mathbf{S}\rangle^2 + 6\langle \mathbf{L}\cdot\mathbf{S}\rangle - 4\langle \mathbf{S}^2\rangle\langle \mathbf{L}^2\rangle}{2(2L-1)(2L+3)} = \begin{cases} -1/5 & (^3P_2)\ , \\ 1 & (^3P_1)\ , \\ -2 & (^3P_0)\ , \end{cases}$$

$$\langle \mathbf{S}_1\cdot\mathbf{S}_2\rangle = \frac{2\langle \mathbf{S}^2\rangle - 3}{4} = \begin{cases} 1/4 & (^3S_1)\ , \\ -3/4 & (^1S_0)\ . \end{cases} \tag{1.9}$$

For example, these expectation values imply the following mass relations for the triplet P states:

$$\begin{aligned} m(^3P_2) &= \bar{m} + m_{\rm s-o} - \frac{1}{5}m_{\rm ten}\ , \\ m(^3P_1) &= \bar{m} - m_{\rm s-o} + m_{\rm ten}\ , \\ m(^3P_0) &= \bar{m} - 2m_{\rm s-o} - 2m_{\rm ten}\ . \end{aligned} \tag{1.10}$$

The mass formulae in Eq. (1.10) can be used to test whether the long-range confining potential transforms as a four-scalar (V_S) or instead as a four-vector (V_V) [BeCDK 79]. For definiteness, we consider a simple modification of the Cornell model in which the 'scalar *vs* vector' issue is cast in terms of a parameter ξ ($0 \le \xi \le 1$),

$$V_S = (1-\xi)br\ , \qquad V_V = \xi br - \frac{a}{r}\ . \tag{1.11}$$

It follows from Eq. (1.7b) and Table XIII–2 that the spin-orbit and tensor mass contributions are then given by

$$\begin{aligned} m_{\rm s-o} &= \frac{1}{2M^2}\left[(4\xi-1)b\langle r^{-1}\rangle + 4a\langle r^{-3}\rangle\right]\ , \\ m_{\rm ten} &= \frac{1}{6M^2}\left[\xi b\langle r^{-1}\rangle + 4a\langle r^{-3}\rangle\right]\ , \end{aligned} \tag{1.12}$$

and upon defining $\lambda \equiv b\langle r^{-1}\rangle / a\langle r^{-3}\rangle$, we form the ratio

$$R \equiv \frac{m(^3P_2) - m(^3P_1)}{m(^3P_1) - m(^3P_0)} = \frac{2}{5}\frac{16 - 19\xi\lambda - 5\lambda}{8 + 5\xi\lambda - \lambda}\ . \tag{1.13}$$

This can be compared with data from the Upsilon P-wave $n = 1, 2$ states,

$$R = \begin{cases} 0.66 & (\eta_b(1P)) \ , \\ 0.70 & (\eta_b(2P)) \ . \end{cases} \tag{1.14}$$

For vector confinement ($\xi \simeq 1$), Eq. (1.13) is in accord with the experimental values of Eq. (1.14) only for $\lambda \simeq 0$, whereas scalar confinement produces reasonable agreement for a much larger range, $0.4 \leq \lambda \leq 1.0$. Moreover, the Cornell model suggests that the latter values for λ are rather more reasonable than the former, and so supports the conclusion that confinement is produced by a long-range, four-scalar interaction.

Transitions in quarkonium

All quarkonium states are unstable. Among the decay mechanisms are annihilation processes, hadronic transitions, and radiative transitions. Roughly speaking, the lightest quarkonium states are relatively narrow, but those lying above the *heavy-flavor threshold*, defined as twice the mass of the lightest heavy-flavored meson and depicted by dashed lines in Figs. XIII–1(a,b), are rather broader. This pattern is particularly apparent for the $^3S_1$ states – below the heavy-flavor threshold, widths are typically tens of keV, whereas above, they are tens of MeV. The primary reason for this difference is that above the heavy-flavor threshold, quarkonium can rapidly 'fall apart' into a pair of heavy-flavored mesons, *e.g.* $\Upsilon[4S] \to B\bar{B}$, whereas below, this mode is kinematically forbidden.

In the following, we shall describe only decays which occur beneath the heavy-flavor threshold, and shall limit our discussion to annihilation processes and hadronic decays. Radiative electric and magnetic dipole transitions are adequately described in quantum mechanics textbooks.

Annihilation transitions: To motivate a procedure for computing annihilation rates in quarkonium, let us consider the simple case of a charged lepton of mass m moving nonrelativistically with its antiparticle in a $^1S_0$ state, and undergoing a transition to a two-photon final state.* First we

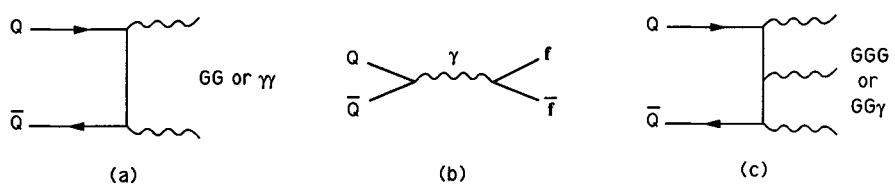

Fig. XIII–4 Decay of quarkonium through annihilation.

* The $^1S_0$ ($^3S_1$) states have even (odd) charge conjugation, and can therefore give rise to even (odd) numbers of photons in an annihilation process.

write down the invariant amplitude for the pair annihilation process,

$$\mathcal{M} = -ie^2\bar{v}(\mathbf{p}_+,\lambda_+)\left[\not\epsilon_2^*\frac{i}{\not p_- - \not q_1 - m}\not\epsilon_1^* + \not\epsilon_1^*\frac{i}{\not p_- - \not q_2 - m}\not\epsilon_2^*\right]u(\mathbf{p}_-,\lambda_-)\ , \tag{1.15}$$

for momentum eigenstates. In the lepton rest frame, we are free to choose, the *transverse gauge* $\epsilon_1^*\cdot p_- = \epsilon_2^*\cdot p_- = 0$, *i.e.* $\epsilon_{1,2}^0 = 0$. Since ${}^3S_1$ states can make no contribution to the two-photon mode, we can compute the squared-amplitude for a ${}^1S_0$ transition by summing over over initial state spins,

$$\sum_{\lambda_\pm}|\mathcal{M}|^2 = \frac{e^4}{2m^2}\left[2 + \frac{\omega_1}{\omega_2} + \frac{\omega_2}{\omega_1} - 4(\boldsymbol{\epsilon}_1^*\cdot\boldsymbol{\epsilon}_2^*)^2\right]\ , \tag{1.16}$$

where $\omega_{1,2}$ are the photon energies in the lepton rest frame. Near threshold the photons emerge back to back, and the differential cross section is found to be

$$\frac{d\sigma}{d\Omega} = \frac{\alpha^2}{2m^2v_+}(1 - (\boldsymbol{\epsilon}_1^*\cdot\boldsymbol{\epsilon}_2^*)^2)\ . \tag{1.17}$$

Likewise, near threshold a sum on photon polarizations gives

$$\sum_{\sigma_{1,2}}(1 - (\boldsymbol{\epsilon}_1^*\cdot\boldsymbol{\epsilon}_2^*)^2)_{\rm thr} = 2\ , \tag{1.18}$$

and upon integrating over half the solid angle (due to photon indistinguishability) we obtain the cross section,

$$\sigma = \frac{4\alpha^2\pi}{m^2v_+}\ . \tag{1.19}$$

This is the transition rate per incident flux of antileptons. Since the flux is just the antilepton velocity v_+ times a unit lepton density, we interpret $v_+\bar{\sigma}$ as the transition rate for a density of *one* lepton per volume. For a bound state with radial quantum number n and wavefunction $\Psi_n(\mathbf{x})$, the density is $|\Psi_n(0)|^2$ and the lowest-order expression for the electromagnetic decay rate $\Gamma_{\gamma\gamma}^{(\rm em)}[{}^1S_0]$ becomes

$$\Gamma_{\gamma\gamma}^{(\rm em)}[{}^1S_0] = v_+\bar{\sigma}|\Psi_n(0)|^2 = \frac{4\pi\alpha^2}{m^2}|\Psi_n(0)|^2\ . \tag{1.20}$$

The corresponding rate for $\gamma\gamma$ emission from ${}^1S_0$ states of the $b\bar{b}$ (Υ) system is obtained from Eq. (1.20) by including a factor $e_b^4 = 1/81$, which accounts for the b-quark charge, and a color factor of three. Determination of the two-gluon emission is found similarly (*cf.* Fig. XIII–4(a)) provided the gluons are taken to be massless free particles, and is left for a problem at the end of the chapter. Including also the effects of

QCD radiative corrections, referred to a common renormalization point $\mu_R = m_b$, we have [KwQR 87]

$$\Gamma_{\Upsilon\to\gamma\gamma}[n^1S_0] = \frac{48\pi\alpha^2|\Psi_n(0)|^2}{81(2m_b)^2}\left[1-3.4\frac{\alpha_s(m_b)}{\pi}\right] ,$$
$$\Gamma_{\Upsilon\to gg}[n^1S_0] = \frac{32\pi\alpha_s^2(m_b)|\Psi_n(0)|^2}{3(2m_b)^2}\left[1+4.4\frac{\alpha_s(m_b)}{\pi}\right] . \quad (1.21)$$

Decays can also occur from the n^3S_1 states.* The single photon intermediate state of Fig. XIII–4(b) leads to emission of a lepton pair, whereas Fig. XIII–4(c) describes final states consisting of three gluons, two gluons and a photon, or three photons. For such a three-particle final state, there are six Feynman diagrams per amplitude and three-particle phase space to contend with. Upon including QCD radiative corrections, the results are [KwQR 87]

$$\Gamma_{\Upsilon\to\ell\bar{\ell}}[n^3S_1] = \frac{16\pi\alpha^2|\Psi_n(0)|^2}{9(2m_b)^2}\left[1-\frac{16}{3}\frac{\alpha_s(m_b)}{\pi}\right] ,$$
$$\Gamma_{\Upsilon\to 3g}[n^3S_1] = \frac{160(\pi^2-9)\alpha_s^3(m_b)|\Psi_n(0)|^2}{81(2m_b)^2}\left[1-4.9\frac{\alpha_s(m_b)}{\pi}\right] ,$$
$$\Gamma_{\Upsilon\to 3\gamma}[n^3S_1] = \frac{64(\pi^2-9)\alpha^3|\Psi_n(0)|^2}{2187(2m_b)^2}\left[1-12.6\frac{\alpha_s(m_b)}{\pi}\right] , \quad (1.22)$$
$$\Gamma_{\Upsilon\to gg\gamma}[n^3S_1] = \frac{128(\pi^2-9)\alpha\alpha_s^2(m_b)|\Psi_n(0)|^2}{81(2m_b)^2}\left[1-1.7\frac{\alpha_s(m_b)}{\pi}\right] .$$

The QCD contributions in Eq. (1.22) are of interest in several respects. They contribute, on the whole, with rather sizeable coefficients and can substantially affect the annihilation rates. Also, they have come to be used as one of several standard inputs for phenomenological determinations of α_s. To eliminate the model-dependent factors $|\Psi_n(0)|^2$, one works with ratios of annihilation rates,

$$\frac{\Gamma_{\Upsilon\to gg\gamma}[n^3S_1]}{\Gamma_{\Upsilon\to 3g}[n^3S_1]} = \frac{4}{5}\frac{\alpha}{\alpha_s(m_b)}\left(1-2.6\frac{\alpha_s(m_b)}{\pi}\right) ,$$
$$\frac{\Gamma_{\Upsilon\to 3g}[n^3S_1]}{\Gamma_{\Upsilon\to\mu\bar{\mu}}[n^3S_1]} = \frac{10}{9}\frac{(\pi^2-9)\alpha_s^3(m_b)}{\pi\alpha^2}\left(\frac{M_\Upsilon}{2m_b}\right)^2\left(1+0.43\frac{\alpha_s(m_b)}{\pi}\right) . \quad (1.23)$$

In reality, there are a number of theoretical and experimental concerns which make the extraction of $\alpha_s(m_b)$ a rather more subtle process than it might at first appear: (i) the contribution of $|\Psi_n(0)|^2$ in Eqs. (1.21),(1.22)

* There are annihilations from higher partial waves as well. These involve derivatives of the wavefunction at the origin.

as a strictly multiplicative factor is a consequence of the nonrelativistic approximation and may be affected by relativistic corrections, (ii) there is no assurance that $\mathcal{O}(\alpha_s)^2$ terms are non-negligible, particularly in the light of the large first order corrections, (iii) experiments see not gluons but rather gluon *jets*, and at the mass scale of the upsilon system, jets are not particularly well-defined, and (iv) the γ spectrum observed in the γgg mode is softer than that predicted by perturbative QCD, implying the presence of important nonperturbative effects. Nevertheless, determinations of this type lead to the central value (and its uncertainties) $\Lambda^{(4)}_{\overline{\rm MS}} = 160^{+100}_{-80}$ MeV as extracted from upsilon data and cited earlier in Table II–3. This example indicates how demanding a task it is to obtain a precise experimental determination of $\alpha_s(q^2)$.

Hadron transitions: The transitions $V' \to V + \pi^0$ and $V' \to V + \eta$ involving the decay of an excited $^3S_1$ quarkonium level (V') down to the $^3S_1$ ground state (V) are interesting because they are forbidden in the limits of flavor $SU(2)$ and $SU(3)$ symmetry respectively. Their rates are therefore governed by quark mass differences, and a ratio of such rates provides a determination of quark mass ratios. There is a modest theoretical subtlety in extracting the rates, as degenerate perturbation theory must be used [IoS 80]. The leading-order effective lagrangian for these P-wave transitions must be linear in the quark mass matrix $\mathbf{m}$,

$$\begin{aligned}\mathcal{L}_{\rm VVM} &= -i\frac{c}{2\sqrt{2}} F_\pi \,{\rm Tr}\left(\mathbf{m}(U - U^\dagger)\right) \epsilon^{\mu\nu\alpha\beta}\partial_\mu V_\nu \partial_\alpha V'_\beta \\ &= c\,[(m_d - m_u)\frac{\pi_3}{\sqrt{2}} + (2m_s - m_d - m_u)\frac{\eta_8}{\sqrt{6}} + \ldots]\epsilon^{\mu\nu\alpha\beta}\partial_\mu V_\nu \partial_\alpha V'_\beta \ ,\end{aligned} \tag{1.24}$$

where c is a constant. Here, π_3 and η_8 are the pure $SU(3)$ states which appear prior to mixing

$$\pi^0 = \cos\theta\ \pi_3 + \sin\theta\ \eta_8 \ , \qquad \eta = -\sin\theta\ \pi_3 + \cos\theta\ \eta_8 \ , \tag{1.25}$$

where $\tan\theta \simeq \theta = \sqrt{3}(m_d - m_u)/[2(2m_s - m_d - m_u)]$ describes the quark mixing. Upon calculating the transition amplitudes and then substituting for the small mixing angle θ, we obtain

$$\begin{aligned}\mathcal{M}_{V'\to V\pi^0} &= \frac{\mathcal{M}_0}{\sqrt{2}}\left[m_d - m_u + \frac{2m_s - m_d - m_u}{\sqrt{3}}\theta\right] = \frac{3\mathcal{M}_0}{2\sqrt{2}}(m_d - m_u) \ , \\ \mathcal{M}_{V'\to V\eta^0} &= \frac{\mathcal{M}_0}{\sqrt{2}}\left[(m_d - m_u)\theta + \frac{2m_s - m_d - m_u}{\sqrt{3}}\right] \\ &= \frac{2\mathcal{M}_0}{\sqrt{6}}(m_s - \hat{m}) + \mathcal{O}\left(\frac{(m_d - m_u)^2}{m_s}\right) \ ,\end{aligned} \tag{1.26}$$

where $\mathcal{M}_0 \equiv ic\,\epsilon^{\mu\nu\alpha\beta}k_\mu\epsilon^*_\nu k'_\alpha\epsilon_\beta$. The ratio of decay rates is found to be

$$\Omega \equiv \frac{\Gamma_{V'\to V\pi^0}}{\Gamma_{V'\to V\eta}} = \frac{27}{16}\left|\frac{m_d - m_u}{m_s - \hat{m}}\right|^2\left|\frac{\mathbf{p}_\pi}{\mathbf{p}_\eta}\right|^3 \quad . \tag{1.27}$$

We can extract a quark mass ratio from charmonium data involving $\psi(2S) \to J/\psi$ transitions. From the measured value $\Omega = 0.037 \pm 0.009$ [RPP 90], we find

$$\frac{m_d - m_u}{m_s - \hat{m}} = 0.0336 \ \pm \ 0.004 \quad , \tag{1.28}$$

which is about 40% larger than the same ratio extracted from pion and kaon masses (*cf.* Eq. (VII–1.10)).

XIII-2 Light mesons and baryons

In the quark model, the light baryons and mesons are Q^3 and $Q\bar{Q}$ combinations of the u, d, s quarks. The resulting spectrum is very rich, containing both orbital and radial excitations of the $L = 0$ ground state hadrons. For mesons, the Q and $\bar{Q}$ spins couple to the total spins $S = 0, 1$, and each $(\mathbf{L}, \mathbf{S})$ combination occurs in the nine flavor configurations of the flavor-$SU(3)$ multiplets **8**, **1**. Analogous statements can be made for baryon states.

In the face of such complex spectra, we are mainly interested in the regularities that allow us to extract the essential physics. A tour through the data base in [RPP 90] reveals some general patterns.* Both radial and orbital excitations of the light hadrons appear $0.5 \to 0.7$ GeV above the ground states. As pointed out in Sect. XI–1, this indicates that the light quarks move relativistically. Other striking regularities are (i) the existence of quasi-degenerate *supermultiplets* of particles with differing flavors and equal (or adjoining) spins, and (ii) excitations of a given flavor having increasingly large mass (M) and angular momentum (J) values which obey $J = \alpha' M^2 + J_0$.

SU(6) classification of the light hadrons

To the extent that the potential is spin-independent and we work in the limit of equal u, d, s mass, the quark hamiltonian is invariant under flavor-$SU(3)$ and spin-$SU(2)$ transformations. To lowest order, hadrons are thus placed in irreducible representations of $SU(6)$, and quarks are assigned to the fundamental representation **6**,

$$\mathbf{6} = (u\uparrow \quad d\uparrow \quad s\uparrow \quad u\downarrow \quad d\downarrow \quad s\downarrow) \quad . \tag{2.1}$$

* Our discussion will focus on hadron masses. Strong and electromagnetic transitions are described in [LeOPR 88].

We can also write the $SU(6)$ quark multiplet in terms of the $SU(3)$ flavor representation and the spin multiplicity as $\mathbf{6} = (\mathbf{3}, 2)$. Although the $SU(6)$ invariant limit forms a convenient basis for a classification of the meson and baryon states, it cannot be a full symmetry of Nature since the spin is a spacetime property of particles whereas $SU(3)$ flavor symmetry is not. Thus it is impossible to unite the flavor and spin symmetries in a relativistically invariant manner [CoM 67]. Although we shall avoid making detailed predictions based on $SU(6)$, it is nonetheless useful in organizing the multitude of observed hadronic levels.

Meson supermultiplets: The L=0 $Q\bar{Q}$ composites are contained in the $SU(6)$ group product $\mathbf{6} \times \mathbf{6}^* = \mathbf{35} \oplus \mathbf{1}$, where the representations **35**, **1** have flavor-spin content

$$\mathbf{35} = (\mathbf{8}, 3) \oplus (\mathbf{8}, 1) \oplus (\mathbf{1}, 3) \ , \qquad \mathbf{1} = (\mathbf{1}, 1) \ . \tag{2.2}$$

The L=0 ground state consists of a vector octet, a pseudoscalar octet, a vector singlet, and a pseudoscalar singlet. For excited states, the meson supermultiplets constitute an $SU(6) \times O(3)$ spectrum of particles. The $O(3)$ label refers to how the total angular momentum is obtained from $\mathbf{J} = \mathbf{L} + \mathbf{S}$, giving rise to the pattern of rotational excitations displayed previously in Table XI–3. Roughly speaking, mesons occur in mass bands having a common degree of radial and/or orbital excitation.

Fig. XIII–5 provides a view of the mass spectrum for the lightest mesons. The $SU(6) \times O(3)$ structure of the ground state and a sequence of orbitally excited states are observed to the extent that sufficient data is available for particle assignments to be made. Note that the S-wave $Q\overline{Q}$ states are all accounted for, but gaps appear in all higher partial waves. Even after many years of study, meson phenomenology below 2 GeV is far from complete!

Baryon supermultiplets: The $SU(6)$ baryon multiplet structure arises from the Q^3 group product $(\mathbf{6}\times\mathbf{6})\times\mathbf{6} = (\mathbf{21}\oplus\mathbf{15})\times\mathbf{6} = \mathbf{56}\oplus\mathbf{70}\oplus\mathbf{70}\oplus\mathbf{20}$, and has flavor-spin content

$$\begin{aligned} \mathbf{56} &= (\mathbf{10}, 4) \oplus (\mathbf{8}, 2) \ , \\ \mathbf{70} &= (\mathbf{8}, 4) \oplus (\mathbf{10}, 2) \oplus (\mathbf{8}, 2) \oplus (\mathbf{1}, 2) \ , \\ \mathbf{20} &= (\mathbf{8}, 2) \oplus (\mathbf{1}, 4) \ . \end{aligned} \tag{2.3}$$

A three-quark system must adhere to the constraint of Fermi statistics. Each baryon state vector is thus antisymmetric under the interchange of any two quarks. A Young-tableaux analysis of the above group product reveals that the spin-flavor parts of the **56**, **70**, and **20** multiplets are respectively symmetric, mixed, and antisymmetric under interchange of pairs of quarks. Since the color part of any Q^3 color-singlet state vector

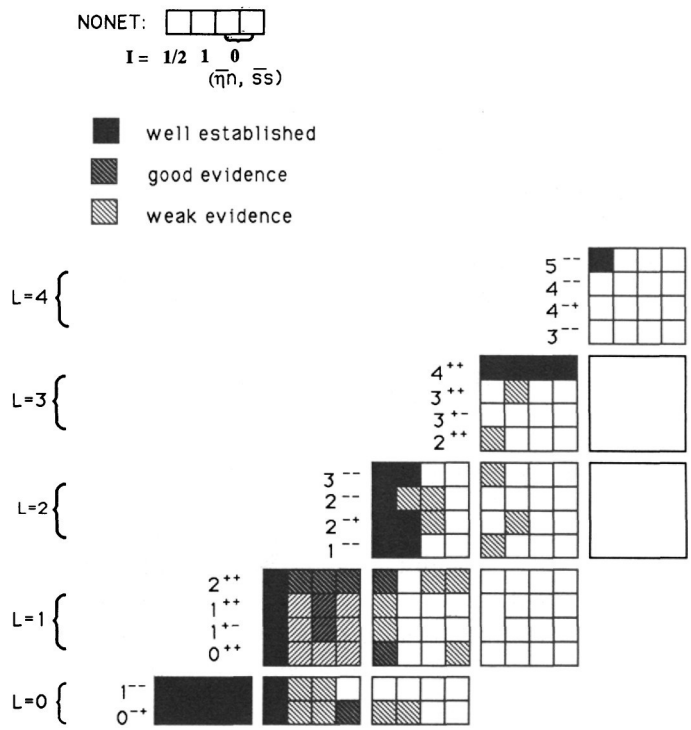

Fig. XIII–5 Spectrum of the light mesons

is antisymmetric under interchange of any two quarks, the **56**-plet has a totally symmetric space wavefunction, with zero orbital angular momentum between each quark-pair. The **70** and **20** multiplets require either radial excitations and/or orbital excitations. Recall the characterization of the baryon spectrum in terms of the basis defined by an independent pair of oscillators (*cf.* Eq. (XI–2.12)). In this context, a standard notation for a baryon supermultiplet is $(\mathbf{R}, L_N^{\mathcal{P}})$, where $\mathbf{R}$ labels the $SU(6)$ representation, $\mathcal{P}$ is the parity, N labels the number of oscillator quanta and L is the orbital angular momentum quantum number (*cf.* Sect. XI–2).

Like meson masses, baryon masses tend to cluster in bands having a common value of N. The first three bands are shown in Fig. XIII–6, and effects of $SU(6)$ breaking are displayed for the first two. The lowest lying $SU(6) \times O(3)$ supermultiplet is the positive parity $(\mathbf{56}, 0_0^+)$, having content as in Eq. (2.3). Next comes the negative parity $(\mathbf{70}, 1_1^-)$ supermultiplet. This contains more states than the 70-plet shown in Eq. (2.3) because the extension from $L = 0$ to $L = 1$ requires addition of

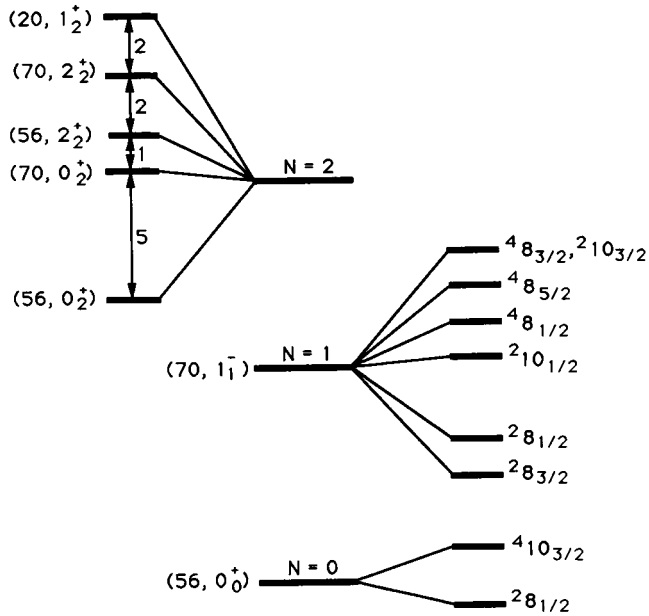

Fig. XIII–6 The low-lying baryon spectrum.

angular momenta,

$$\begin{aligned} (\mathbf{10},2) &\to (\mathbf{10},4) \frown (\mathbf{10},2)\ , \quad & (\mathbf{8},4) &\to (\mathbf{8},6) \frown (\mathbf{8},4) \frown (\mathbf{8},2)\ , \\ (\mathbf{1},2) &\to (\mathbf{1},4) \frown (\mathbf{1},2)\ , & (\mathbf{8},2) &\to (\mathbf{8},4) \frown (\mathbf{8},2)\ . \end{aligned} \tag{2.4}$$

The number of supermultiplets grows per unit of excitation thereafter. There are five $SU(6)$ multiplets in the $N = 2$ band, $(\mathbf{56}, 2_2^+)$, $(\mathbf{56}, 0_2^+)$, $(\mathbf{70}, 2_2^+)$, $(\mathbf{50}, 0_2^+)$, and $(\mathbf{20}, 1_2^+)$. Recall that the baryonic inter-quark potential was expressed in Eq. (XI–2.10) as $V = V_{\rm osc} + U$, where $V_{\rm osc}$ is the potential energy of a harmonic oscillator and $U \equiv V - V_{\rm osc}$. If the potential energy were purely $V_{\rm osc}$, the supermultiplets within the $N = 2$ band would all be degenerate. In the potential model, assuming that the largest part of U is purely radial, this degeneracy is removed by the first-order perturbative effect of U, and the splittings in the $N = 2$ band are shown at the top of Fig. XIII–6. Aside from choosing the $(\mathbf{56}, 0_2^+)$ supermultiplet to have the lowest mass, one finds the pattern of splitting to be as shown in Fig. XIII–6, *independent* of the particular form of U [HeK 83].

Regge trajectories

It is natural to classify together a ground state hadron and its rotational excitations, *e.g.* the isospin one-half baryons $N(939)_{J=1/2}$ (the nucleon), $N(1680)_{J=5/2}$, and $N(2220)_{J=9/2}$. Although no higher spin entries have

been detected in this particular set of nucleonic states (presumably due to experimental limitations), there is no theoretical reason to expect any such sequence to end. The data base in [RPP 90] contains a number of similar structures, each characteristically containing three or four members.

Each such collection of states is said to belong to a given *Regge trajectory*. To see how this concept arises, let us consider the simplest case of two spinless particles with scattering amplitude $f(E,z)$ (*i.e.* $d\sigma/d\Omega = |f(E,z)|^2$), where E is the energy and $z = \cos\theta$ is the scattering angle. It turns out that analytic properties of the scattering amplitude in the complex angular momentum (J) plane are of interest. One may obtain a representation of $f(E,z)$ in the complex J-plane by converting the partial wave expansion into a so-called *Watson-Sommerfeld transform*,

$$\begin{aligned} f(E,z) &= \sum_{\ell=0}^{\infty} (-)^{\ell}(2\ell+1)a(E,\ell)P_{\ell}(-z) \\ &\to \frac{1}{2\pi i}\oint_{\mathcal{C}} dJ\ \frac{\pi}{\sin\pi J}(2J+1)a(E,J)P_J(-z)\ , \end{aligned} \tag{2.5}$$

where P_ℓ is a Legendre polynomial and $\mathcal{C}$ is a contour enclosing the non-negative integers. Suppose that as $\mathcal{C}$ is deformed away from the Re J axis to, say, a line of constant Re J, a pole in the partial wave amplitude $a(E,J)$ is encountered. Such a singularity is referred to as a *Regge pole* and contributes (*cf.* Eq. (2.5)) to the full scattering amplitude as

$$f(E,z) = \frac{\beta[E]P_{\alpha[E]}(-z)}{\sin(\pi\alpha[E])} + \dots\ , \tag{2.6}$$

where $\alpha[E]$ is the energy-dependent pole position in the complex J-plane and $\beta[E]$ is the pole residue.

Table XIII–3. Regge trajectories.

Trajectory	N	Slope[a]	J-intercept
N	3	0.99	−0.34
Δ	3	0.92	0.07
Λ	3	0.94	−0.64
Σ	3	1.1	−1.2
Σ^*	2	0.91	−0.24
π	3	0.72	−0.05
ρ	4	0.84	0.54
K	4	0.69	−0.22
K^*	4	0.86	0.29

[a] In units of GeV^{-2}

The Regge-pole contribution of Eq. (2.6) can manifest itself physically in both the direct channel as a resonance and a crossed channel as an exchanged particle. Here, we discuss just the former case by demonstrating how a given Regge pole can be related to a *sequence* of rotational excitations. Suppose that at some energy E_R, the real part of the pole position equals a nonnegative integer ℓ, *i.e.* Re $\alpha[E_R] = \ell$. Then with the aid of the identity,

$$\frac{1}{2}\int_{-1}^{1} dz\ P_\ell(z)P_\alpha(-z) = \frac{1}{\pi}\frac{\sin(\pi\alpha)}{(\ell-\alpha)(\ell+\alpha+1)}\quad , \tag{2.7}$$

we can infer from Eq. (2.6) the Breit-Wigner resonance form

$$a_\ell^{(\mathrm{Rg.-ple.})} = \frac{\beta}{\pi}\frac{1}{(\alpha[E]-\ell)(\alpha[E]+\ell+1)} \simeq \frac{\Gamma/2}{E-E_R+i\Gamma/2} \tag{2.8}$$

provided Re $\alpha[E_R] \gg$ Im $\alpha[E_R]$. A physical resonance thus appears if $\alpha[E]$ passes near a non-negative integer, and if the Regge pole moves to ever-increasing J values in the complex J-plane as the energy E is increased, it generates a tower of high-spin states. Except in instances of so-called exchange degeneracy, parity dictates that there be two units of angular momentum between members of a given trajectory. In this manner, a single Regge pole in the angular momentum plane gives rise to the collection of physical states called a *Regge trajectory.*

A plot of the angular momentum *vs* squared-mass for the states on any meson or baryon trajectory reveals the linear behavior,

$$J \simeq \alpha' m^2 + J_0\quad . \tag{2.9}$$

A compilation of slopes (α') and intercepts (J_0) appears in Table XIII–3, with each trajectory labeled by its ground state hadron. Such linearly rising trajectories have been interpreted as a consequence of QCD [JoT 76]. In this picture, hadrons undergoing highly excited rotational motion come to approach color-flux tubes, whereupon it becomes possible to relate the angular momentum of rotation to the energy contained in the color field. This line of reasoning leads to the behavior of Eq. (2.9), and accounts for the universality seen in the slope values displayed in Table XIII–3.

SU(6) breaking effects

Although an $SU(6)$ invariant hamiltonian provides a convenient basis for describing light hadrons, the physical spectrum exhibits substantial departures from the mass degeneracies which occur in this overly symmetric picture. In the following, we shall consider some simple models for explaining the many $SU(6)$ breaking effects observed in the real world.

The QCD Breit-Fermi model: If one ascribes the non-confining part of the quark interaction to single-gluon exchange, the nonrelativistic limit

yields the 'QCD Breit-Fermi potential' [DeGG 75]

$$V_{\text{one-gluon}} = -\frac{4k\alpha_s}{3r} + \frac{4k\alpha_s}{3}\sum_{i<j}\left[\frac{8\pi}{3M_iM_j}\mathbf{s}_i\cdot\mathbf{s}_j\delta^3(\mathbf{r}) + \frac{\pi}{2}\delta^3(\mathbf{r})\left(\frac{1}{M_i^2}+\frac{1}{M_j^2}\right)\right.$$
$$+\frac{1}{M_iM_jr^3}[3(\mathbf{s}_i\cdot\hat{\mathbf{r}})(\mathbf{s}_j\cdot\hat{\mathbf{r}})-\mathbf{s}_i\cdot\mathbf{s}_j]$$
$$+\frac{1}{r^3}\left(\frac{\mathbf{s}_i\cdot\mathbf{r}\times\mathbf{p}_i}{2M_i^2}-\frac{\mathbf{s}_j\cdot\mathbf{r}\times\mathbf{p}_j}{2M_j^2}-\frac{\mathbf{s}_j\cdot\mathbf{r}\times\mathbf{p}_i-\mathbf{s}_i\cdot\mathbf{r}\times\mathbf{p}_j}{M_iM_j}\right)$$
$$\left.+\frac{1}{2M_iM_jr}(\mathbf{p}_i\cdot\mathbf{p}_j+\hat{\mathbf{r}}(\hat{\mathbf{r}}\cdot\mathbf{p}_i)\cdot\mathbf{p}_j)\right] , \qquad (2.10)$$

where α_s is the strong fine structure constant, $\mathbf{r}\equiv\mathbf{r}_{ij}$, and k denotes the color dependence of the potential (*cf.* Sect. XI–2) with $k=1$ (1/2) for mesons (baryons). In keeping with the potential model, the mass parameters $\{M_i\}$ are interpreted as constituent quark masses. Although the QCD Breit-Fermi model incorporates $SU(6)$ breaking by means of both quark mass splittings and spin-dependent interactions, it lacks a rigorous theoretical foundation. One might argue on the grounds of asymptotic freedom that Eq. (2.10) does justice to physics at very short distances (in the approximation that α_s is constant), but there is no reason to believe that it suffices at intermediate length scales. It also does not account for mixing between isoscalar mesons, so such states must be considered separately.

Meson masses: The gluon-exchange model can be used to obtain information on constituent quark mass. In the following, we shall temporarily ignore the minor effect of isospin breaking by working with $\hat{M}\equiv(M_u+M_d)/2$. To compute meson masses, we take the expectation value of the full hamiltonian between $SU(6)$ eigenstates, specifically the $L=0$ $Q\bar{Q}$ states.* Although the form of Eq. (2.10) implies the presence of spin-spin, spin-orbit, and tensor interactions, the spin-orbit and tensor terms do not contribute here because each quark pair moves in an S-wave, and it is the spin-spin (hyperfine) interaction which lifts the vector meson states relative to the pseudosclar mesons. We can parameterize the non-isoscalar $L=0$ meson masses as

$$m_{Q\bar{Q}}^{(L=0)} = \hat{n}\hat{M} + n_sM_s + \frac{\langle\mathbf{p}_Q^2\rangle}{2M_Q} + \frac{\langle\mathbf{p}_{\bar{Q}}^2\rangle}{2M_{\bar{Q}}} + \mathcal{H}_{Q\bar{Q}}\langle\mathbf{s}_Q\cdot\mathbf{s}_{\bar{Q}}\rangle , \qquad (2.11)$$

* An analysis of spin-dependence in the $L=1$ states is the subject of a problem at the end of the chapter (*cf.* Prob. XIII-3)).

where $\hat{n}$ and n_s are the number of nonstrange and strange consituents respectively, and $\mathcal{H}_{Q\bar{Q}}$ is the hyperfine mass parameter defined in Eq. (XII–3.12).

One consequence of Eq. (2.11) is a relation involving the mass ratio $\hat{M}/M_s$. Fitting the four masses $\pi(138)$, $K(496)$, $\rho(770)$, $K^*(892)$ to the parameters in Eq. (2.11) yields

$$\frac{m_{K^*} - m_K}{m_\rho - m_\pi} = \frac{\mathcal{H}_{\rm ns}}{\mathcal{H}_{\rm nn}} = \frac{\hat{M}}{M_s} \simeq 0.63 \quad . \tag{2.12}$$

The origin of this result lies in the inverse dependence of the hyperfine interaction upon constituent quark mass, which affects the mass splitting between $S = 1$ and $S = 0$ mesons differently for strange and nonstrange mesons. The numerical value of $\hat{M}/M_s$ in Eq. (2.12) graphically demonstrates the difference between constituent quark masses and current quark masses, the latter having a mass ratio of about 0.04 (*cf.* Eq. (VII–1.6a)). In earlier sections of this book which stressed the role of chiral symmetry, the pion was given a special status as a quasi-Goldstone particle. In the $Q\bar{Q}$ model, the small pion mass is seen to be a consequence of severe cancelation between the spin-independent and spin-dependent contributions. However, the parameterization of Eq. (2.11) cannot explain the large $\eta'(960)$ mass.

In addition to the $SU(6)$ symmetry breaking effects of mass and spin, there is an additive contribution present in the isoscalar channel which is induced by quark-antiquark annihilation into gluons. In the basis of u, d, s quark flavor states, this annihilation process produces a 3×3 mass matrix of the form

$$\begin{pmatrix} 2M_u + X & X & X \\ X & 2M_d + X & X \\ X & X & 2M_s + X \end{pmatrix} \tag{2.13}$$

where for $C = +1(-1)$ mesons, X is the two-gluon (three-gluon) annihilation amplitude, and for simplicity we display just the quark mass contribution $(2M_i)$ as the nonmixing mass contribution. The annihilation process is a short-range phenomenon, so the magnitude of X depends sharply on the orbital angular momentum L of the $Q\bar{Q}$ system. For $L \neq 0$ waves (where the wavefunction vanishes at zero relative separation), and $C = -1$ channels (where the annihilation amplitude is suppressed by the three powers of gluon coupling), we expect $M_s - \hat{M} \gg X$. In this limit, diagonalization of Eq. (2.13) yields to leading order the set of basis states $(\bar{u}u \pm \bar{d}d)/\sqrt{2}$ and $\bar{s}s$. Only the $L = 0$ pseudoscalar channel experiences opposite limit $X \gg M_s - \hat{M}$, wherein to leading order the basis vectors are the $SU(3)$ singlet state $(\bar{u}u + \bar{d}d + \bar{s}s)/\sqrt{3}$ and octet states $(\bar{u}u - \bar{d}d)/\sqrt{2}$, $(\bar{u}u + \bar{d}d - 2\bar{s}s)/\sqrt{6}$. The overall picture that emerges is one of relatively

unmixed light pseudoscalar states, and heavily mixed vector, tensor, *etc.* states.

Baryon masses: Applying the one-gluon exchange potential to the ground state baryons of $(\mathbf{56}, 0_0^+)$ yields a mass formula analogous to Eq. (2.11),

$$m_{Q^3}^{(L=0)} = \hat{n}\hat{M} + n_s M_s + \sum_{i=1}^{3} \frac{\langle \mathbf{p}_i^2 \rangle}{2M_i} + \frac{1}{2}\sum_{i<j} \mathcal{H}_{ij} \langle \mathbf{s}_i \cdot \mathbf{s}_j \rangle \quad . \tag{2.14}$$

For the system of $1/2^+$ and $3/2^+$ (iospin-averaged) baryons, there are eight mass values and since the above mass formula contains five parameters, one should obtain three relations. The additional perturbative assumption $\mathcal{H}_{ss} - \mathcal{H}_{ns} = \mathcal{H}_{ns} - \mathcal{H}_{nn}$ for the hyperfine mass parameters yields the well-known Gell-Mann–Okubo relation of Eq. (XII–3.10) for the $1/2^+$ baryons and the *equal spacing rule* for $3/2^+$ states,

$$\begin{gathered} m_{\Sigma^*} - m_\Delta = m_{\Xi^*} - m_{\Sigma^*} = m_\Omega - m_{\Xi^*} \quad . \\ (\text{Expt. } 153 \text{ MeV } = \ 149 \text{ MeV } = \ 139 \text{ MeV }) \end{gathered} \tag{2.15}$$

A third relation which relates the $3/2^+$ and $1/2^+$ masses and is independent of further perturbative assumptions has the form

$$\begin{gathered} 3m_\Lambda - m_\Sigma - 2m_N = 2(m_{\Sigma^*} - m_\Delta) \\ (\text{Expt.}: \quad 276 \text{ MeV} = 305 \text{ MeV}) \end{gathered} \tag{2.16}$$

In addition, one can obtain estimates for $\hat{M}/M_s$, among them

$$\begin{aligned} \frac{\hat{M}}{M_s} &= \frac{2(m_{\Sigma^*} - m_\Sigma)}{2m_{\Sigma^*} + m_\Sigma - 3m_\Lambda} \simeq 0.62 \quad , \\ \frac{\hat{M}}{M_s} &= \frac{m_{\Sigma^*} - m_\Sigma}{m_\Delta - m_N} \simeq 0.65 \quad , \end{aligned} \tag{2.17}$$

both in accord with Eq. (2.12).

Isospin breaking effects: The above description of $SU(6)$ breaking assumes isospin conservation. In fact, hadrons exhibit small mass splittings within isospin multiplets, arising from electromagnetism and the $u - d$ mass difference. In the pion and kaon systems, we were able to use chiral $SU(3)$ symmetry to isolate each of these separately. Unfortunately, this is not possible in general, and models are required to address this issue.

There are a few consequences which follow purely from symmetry considerations. Since the mass difference $m_u - m_d$ is $\Delta I = 1$, the $\Delta I = 2$ combinations

$$m_{\Sigma^+} + m_{\Sigma^-} - 2m_{\Sigma^0} = 1.7 \pm 0.1 \text{ MeV} \ , \quad m_{\rho^+} - m_{\rho^0} = -0.3 \pm 2.2 \text{ MeV} \ , \tag{2.18}$$

arise only from the electromagnetic interaction. In addition, both electromagnetic and quark mass contributions satisfy the *Coleman-Glashow relation* [CoG 64],

$$\begin{aligned} m_{\Sigma^+} - m_{\Sigma^-} + m_n - m_p + m_{\Xi^-} - m_{\Xi^0} = 0 \\ [\text{Expt. } 0.4 \pm 0.6 \text{ MeV} = 0\ ]\ . \end{aligned} \tag{2.19}$$

For electromagnetism, this is a consequence of the U-spin singlet character of the current, whereas for quark masses it follows from the $\Delta I = 1$ and $SU(3)$-octet character of the current.

We proceed further by using a simple model, based on the QED coulomb and hyperfine effects, to describe the electromagnetic interaction of quarks,

$$\begin{aligned} \Delta m_{\text{coul}} &= \mathcal{A}_{\text{coul}} \sum_{i<j} Q_i Q_j\ , \\ \Delta m_{\text{hyp}} &= -\mathcal{A}_{\text{hyp}} \sum_{i<j} \frac{Q_i Q_j}{M_i M_j} \mathbf{s}_i \cdot \mathbf{s}_j\ , \end{aligned} \tag{2.20}$$

where $\mathcal{A}_{\text{coul}}$, $\mathcal{A}_{\text{hyp}}$ are constants, $\{Q_i\}$ are quark electric charges, and the sums are taken over constituent quarks. In Δm_{hyp}, we shall neglect further isospin breaking in the masses and use $M_u = M_d = \hat{M}$, and assume electromagnetic self-interactions of a quark to be already accounted for in the mass parameter of that quark. For any values of $\mathcal{A}_{\text{coul}}$ and $\mathcal{A}_{\text{hyp}}$, this model contains the sum rule

$$(m_n - m_p)_{\text{em}} = -\frac{1}{3}(m_{\Sigma^+} + m_{\Sigma^-} - 2m_{\Sigma^0}) = -0.57 \pm 0.03 \text{ MeV}\ , \tag{2.21}$$

leaving the excess due to the quark mass difference,

$$\begin{aligned} (m_n - m_p)_{\text{qm}} &= \frac{m_u - m_d}{2} \cdot \langle n|\bar{u}u - \bar{d}d|n\rangle - \frac{m_u - m_d}{2} \cdot \langle p|\bar{u}u - \bar{d}d|p\rangle \\ &\equiv (m_d - m_u)(d_m + f_m) Z_0 \\ &= (m_n - m_p) - (m_n - m_p)_{\text{em}} = 1.86 \pm 0.03 \text{ MeV}\ , \end{aligned} \tag{2.22}$$

where the second line in the above uses the parameterization of hyperon mass splittings given in Eq. (XII–3.8). To the extent that this estimate of quark mass differences is meaningful, one obtains the mass ratio,

$$\frac{m_d - m_u}{m_s - \hat{m}} = \frac{(m_n - m_p)_{\text{qm}}}{m_\Xi - m_\Sigma} \simeq 0.015\ , \tag{2.23}$$

to be compared to the chiral-symmetry extraction from meson masses which yielded 0.023 (*cf.* Eq. (VII–1.10)). With further neglect of terms $\mathcal{O}(\alpha(M_s - \hat{M}))$ in the hyperfine interaction, this exercise can be repeated

for vector mesons to yield

$$\begin{aligned}(m_{K^{*0}} - m_{K^{*+}})_{\rm em} &= -\frac{2}{3}(m_{\rho^+} - m_{\rho^0}) = 0.2 \pm 1.5 \text{ MeV} , \\ (m_{K^{*0}} - m_{K^{*+}})_{\rm qm} &= (m_{K^{*0}} - m_{K^{*+}}) - (m_{K^{*0}} - m_{K^{*+}})_{\rm em} \\ &= 6.5 \pm 1.9 \text{ MeV} , \\ \frac{m_d - m_u}{m_s - \hat{m}} &= \frac{m_{K^{*0}} - m_{K^{*+}}}{m_{K^*} - m_\rho} = 0.053 \pm 0.016 .\end{aligned} \tag{2.24}$$

The additional assumption that the constants $\mathcal{A}_{\rm coul}$ and $\mathcal{A}_{\rm hyp}$ are the *same* in the decuplet baryons and the octet baryons, as is true in the $SU(6)$ limit, leads to

$$\begin{aligned}(m_{\Delta^{++}} - m_{\Delta^0})_{\rm em} &= \frac{5}{3}(m_{\Sigma^+} + m_{\Sigma^-} - 2m_{\Sigma^0}) = 2.8 \pm 0.2 \text{ MeV} , \\ (m_{\Delta^{++}} - m_{\Delta^0})_{\rm qm} &= (m_{\Delta^{++}} - m_{\Delta^0}) - (m_{\Delta^{++}} - m_{\Delta^0})_{\rm em} \\ &= -5.5 \pm 0.4 \text{ MeV} , \\ \frac{m_d - m_u}{m_s - \hat{m}} &= \frac{1}{2}\frac{m_{\Delta^0} - m_{\Delta^{++}}}{m_{\Sigma^*} - m_\Delta} = 0.018 \pm 0.002 .\end{aligned} \tag{2.25}$$

Of course, the spread of values for the mass ratios raises a concern about the validity of this simple model. However, all methods of calculation agree on the smallness of the ratio $(m_d - m_u)/(m_s - \hat{m})$.

XIII-3 The heavy-quark limit

In the quark description, a heavy-flavored hadron contains at least one of the heavy quarks c, b, t. It is possible to describe such heavy systems with dynamical models like those employed for the light hadrons [DeGG 75, IzDS 82]. However, while such models are often valuable, it is always preferable to have a valid approximation scheme which follows *directly* from QCD. In this regard, a study of the heavy-quark limit ($m_Q \to \infty$) in which the theory is expanded in powers of m_Q^{-1} is proving useful in analytic and lattice studies of meson spectroscopy and in the area of weak decays.

Heavy-flavored hadrons in the quark model

The spectroscopy of heavy-flavored hadrons should qualitatively follow that of the light hadronic spectrum, with states containing a single heavy-quark Q occurring as either mesons ($Q\bar{q}$) or baryons (Qq_1q_2). The lowest energy state for a given hadronic flavor will have zero orbital angular momentum between the quarks, leading to ground state spin values $S = 0, 1$ for mesons and $S = 1/2, 3/2$ for baryons. The hyperfine interaction will lower the $S = 0$ meson and $S = 1/2$ baryon masses, and both orbital and radial hadronic excitations of the ground state will be present.

Although it is possible to contemplate extended flavor transformations which involve interchange of the light and heavy quarks, *e.g.* as in the $SU(4)$ of the light and charmed hadrons, such symmetries are so badly broken by the difference in energy scales $M_Q \gg M_q$ and $M_Q \gg \Lambda_{\rm QCD}$ as to be rendered useless. However, the $SU(3)$ and $SU(2)$ flavor symmetries associated with the light hadrons are still viable, but multiplet patterns become modified. The mesons $Q\bar{q}$ will exist in the $SU(3)$ multiplet $\mathbf{3}^*$, whereas in the baryonic Qq_1q_2 configurations the two light quarks q_1, q_2 will form the flavor $SU(3)$ multiplets $\mathbf{6}$ and $\mathbf{3}^*$. For example, the charmed system has the meson ground state

$$\mathbf{3}^*: \quad D^+[c\bar{d}],\ D^0[c\bar{u}],\ D^s[c\bar{s}] \quad ,$$

which displays the mass pattern of an $SU(2)$ doublet $(D^+_{1869},\ D^0_{1865})$ and an $SU(2)$ singlet (D^s_{1969}). The charmed baryon multiplets are

$$\mathbf{6}: \quad \Sigma_c^{++}[uuc],\ \Sigma_c^{+}[udc],\ \Sigma_c^{0}[ddc],\ \Xi_c^{+(s)}[usc],\ \Xi_c^{0(s)}[dsc],\ \Omega_c^{0}[ssc]$$
$$\mathbf{3}^*: \quad \Lambda_c^{+}[udc],\ \Xi_c^{+a}[usc],\ \Xi_c^{0a}[dsc] \quad .$$

Fig. XIII–7 displays the anticipated charmed meson and charmed baryon levels, including the effect of $SU(3)$ breaking.

Heavy-quark constituent mass values can be inferred from the $D^* - D$ and $B^* - B$ hyperfine splittings. That the former splitting is about three times the latter is a consequence of $M_b \simeq 3M_c$ and of the inverse dependence of the hyperfine effect upon quark mass. Analogously to Eq. (2.17), we find

$$\frac{\hat{M}}{M_c} = \frac{m_{D^*} - m_D}{m_\rho - m_\pi} \simeq 0.22 \ , \qquad \frac{\hat{M}}{M_b} = \frac{m_{B^*} - m_B}{m_\rho - m_\pi} \simeq 0.08 \ , \tag{3.1}$$

where $\hat{M} \equiv (M_u + M_d)/2$. These findings depend to some extent on how the fit is done, *e.g.* with mesons or with baryons, and we leave further study for Prob. XIII–4.

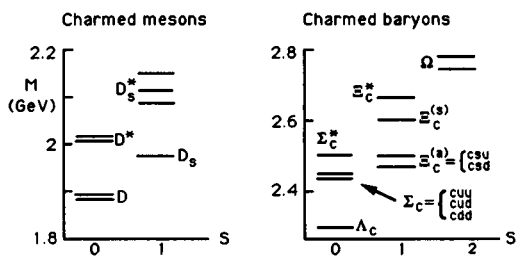

Fig. XIII–7 Spectrum of charmed (a) mesons, (b) baryons

Spectroscopy in the $m_Q \to \infty$ limit

In a hadron which contains a single heavy quark Q along with light degrees of freedom, the heavy quark is essentially static. The best analogy is with atoms, where the nucleus can in the first approximation be treated as a static, electrically-charged source. Likewise, for heavy hadrons the heavy quark is a static source with color charge, and the light degrees of freedom provide a non-static hadronic environment around Q. This scenario can be formalized by partitioning the heavy quark lagrangian as [CaL 86, Ei 88, LeT 88]

$$\begin{aligned} \mathcal{L}_Q &= \bar{\psi}\,(i\not{D} - m_Q)\,\psi \equiv \mathcal{L}_0 + \mathcal{L}_{\rm space} \\ \mathcal{L}_0 &= \bar{\psi}\,(i\gamma_0 D_0 - m_Q)\,\psi\ , \qquad \mathcal{L}_{\rm space} = -i\bar{\psi}\boldsymbol{\gamma}\cdot\mathbf{D}\psi\ , \end{aligned} \tag{3.2}$$

where $D_\mu\psi$ is the covariant derivative of $SU(3)_c$. Since the spatial $\boldsymbol{\gamma}$ matrices connect upper and lower components, we see that the effect of $\mathcal{L}_{\rm space}$ is $\mathcal{O}(m_Q^{-1})$.

Observe that the static lagrangian $\mathcal{L}_0$ of Eq. (3.2) is invariant under spin rotations of the heavy quark Q. In the world defined by $\mathcal{L}_0$, with both $\mathcal{O}(\Lambda_{\rm QCD}/M_Q)$ effects and $\mathcal{O}(\alpha_s(M_Q))$ effects (associated with hard-gluon exchange) ignored, heavy hadronic energy levels and couplings are constrained by the $SU(2)$ spin symmetry. It is helpful to visualize the situation. A heavy flavored hadron of spin $\mathbf{S}$ will contain a static quark Q having a constant spin vector $\mathbf{S}_Q$ (with $S_Q = 1/2$) and light degrees of freedom having a constant angular momentum vector $\mathbf{J}_\ell \equiv \mathbf{S} - \mathbf{S}_Q$.* For a meson of this type, we assume that J_ℓ behaves as it does in the quark model, with $J_\ell = 1/2$ in the ground state and $J_\ell = L \pm 1/2$ for $L > 0$ rotational excitations. From the decoupling of the heavy quark spin, it follows that *there will be a two-fold degeneracy between mesons having spin values* $S = J_\ell \pm 1/2$. The meson $L = 0$ ground state will have $J_\ell = 1/2$ and thus degenerate states with $S = 0, 1$. The $L = 1$ first rotational excitation with $J_\ell = 1/2$ will give rise to degenerate $S = 0, 1$ levels, whereas for $J_\ell = 3/2$ one obtains degenerate levels having $S = 1, 2$. Moreover, the energy differences between different levels should be independent of heavy quark flavor. Analogous conditions hold for heavy flavored baryons and hadronic transitions between levels of differing L can be similarly analyzed.

Let us explicitly demonstrate that the splitting between the $J^P = 1^-$ and $J^P = 0^-$ states of a $Q\bar{q}$ meson must vanish in the limit of infinite quark mass. We note that the mathematical condition for spin-

---

* Although the light degree(s) of freedom in the simple quark model is an antiquark $\bar{q}$ for mesons and two quarks $q_1 q_2$ for baryons, the physical (*i.e.* actual) light degrees of freedom could entail unlimited numbers of gluons and/or quark-antiquark pairs.

independence is

$$\left[H_0, S_3^Q\right] = 0 \quad , \tag{3.3}$$

where S_3^Q is the generator of spin rotations about the 3-axis for quark Q and H_0 is the hamiltonian obtained from $\mathcal{L}_0$. Since the action of S_3^Q on a 0^- state produces a 1^- state, *i.e.* $|M_{1^-}\rangle = 2S_3{}^Q|M_{0^-}\rangle$, we then have

$$H_0|M_{1^-}\rangle = m_{1^-}|M_{1^-}\rangle = 2S_3{}^Q H_0|M_{0^-}\rangle = m_{0^-}|M_{1^-}\rangle \ , \tag{3.4}$$

implying that $m_{1^-} - m_{0^-} \to 0$ as $m_Q \to \infty$.

Another consequence of working in the static limit of $\mathcal{L}_0$ is that the propagator, $S_\infty(x,y)$, of the heavy quark in an external field can be determined exactly. From the defining equations,

$$(i\gamma_0 D_0 - m_Q)\, S_\infty(x,y) = \delta^{(4)}(x-y) \qquad (D_0 \equiv \partial_0 + ig_3 \mathbf{A}_0 \cdot \boldsymbol{\lambda}/2) \ , \tag{3.5}$$

one has the solution

$$\begin{aligned} S_\infty(x,y) = -iP(x_0,y_0)\delta^{(3)}(\mathbf{x}-\mathbf{y}) \Bigg[& \theta(x^0-y^0) e^{-im_Q(x^0-y^0)} \left(\frac{1+\gamma_0}{2}\right) \\ & + \theta(y^0-x^0) e^{im_Q(x^0-y^0)} \left(\frac{1-\gamma_0}{2}\right) \Bigg] \quad , \end{aligned} \tag{3.6}$$

where $P(x_0,y_0)$ is the path-ordered exponential along the time direction,

$$P(x_0,y_0) \equiv P \exp\left[i\frac{g_3}{2} \int_{y^0}^{x_0} dt\, \boldsymbol{\lambda} \cdot \mathbf{A}_0(\mathbf{x},t) \right] \quad . \tag{3.7}$$

In this approximation, the heavy quark is static at point $\mathbf{x}$ and the only time-dependence is that of a phase.

This discussion can be generalized to a frame where the heavy quark is moving at a fixed velocity $\mathbf{v}$, described by a velocity four vector $v^\mu = p^\mu/m_Q$, with $v^\mu v_\mu = 1$. One can define projection operators

$$\Gamma_{v\pm} = \frac{1}{2}\left(1 \pm \not{v}\right) \ , \tag{3.8}$$

where $\Gamma_{v\pm}^2 = \Gamma_{v\pm}$, $\Gamma_{v\pm}\Gamma_{v\mp} = 0$, and $\Gamma_{v+} + \Gamma_{v-} = 1$. The $\Gamma_{v\pm}$ generalize the usual projection of 'upper' and 'lower' components into the moving frame. A quark moving with velocity $\mathbf{v}$ will have the leading description of its wavefunction contained in the 'upper' component described by a field h_v [Ge 90, Wi 91],

$$\Gamma_{v+}\psi \equiv e^{-im_Q v\cdot x} h_v(x) \quad , \tag{3.9}$$

where the main dependence on the quark mass has been factored out, and h_v obviously satisfies $\Gamma_{v+}h_v = h_v$. Substituting into the Dirac lagrangian,

neglecting lower components, and using $\Gamma_{v+} \not{D} \Gamma_{v+} = v \cdot D$ yields

$$\mathcal{L}_Q = \bar{\psi} \left(i \not{D} - m_Q \right) \psi \simeq \bar{\psi} \Gamma_{v+} \left(i \not{D} - m_Q \right) \Gamma_{v+} \psi = \bar{h}_v i v \cdot D h_v \quad , \tag{3.10}$$

which generates the lowest order equation of motion $v \cdot D h_v = 0$. This approximation can be systematically improved by inclusion of a 'lower' component for the heavy-quark field [EiH 90a,b, Lu 90, GeGW 90],

$$\Gamma_{v-} \psi \equiv e^{-i m_Q v \cdot x} \ell_v(x) \quad , \tag{3.11}$$

with $\Gamma_{v-} \ell_v = \ell_v$. The equations of motion allow us to solve for ℓ_v by following the sequence of steps,

$$\begin{aligned} 0 = \left(i \not{D} - m_Q \right) \psi &= \left(i \not{D} - m_Q \right) e^{-i m_Q v \cdot x} \left[h_v + \ell_v \right] \\ &= e^{-i m_Q v \cdot x} \left(m_Q (\not{v} - 1) + i e^{-i m_Q v \cdot x} \not{D} \right) \left[h_v + \ell_v \right] \\ &= e^{-i m_Q v \cdot x} \left[(-2 m_Q + i \not{D}) \ell_v + i \not{D} h_v \right] \quad , \end{aligned} \tag{3.12}$$

which yields l_v and ψ as

$$\begin{aligned} \ell_v &= \frac{i}{2 m_Q} \not{D} h_v + \mathcal{O}(m_Q^{-2}) \\ \psi &= e^{-i m_Q v \cdot x} \left[1 + \frac{i}{2 m_Q} \not{D} \right] h_v + \mathcal{O}(m_Q^{-2}) \quad . \end{aligned} \tag{3.13}$$

Inserting these forms into Eq. (3.10) and using $\Gamma_{v+} h_v = h_v$ and Eq. (III–3.50) for $\not{D} \not{D}$ yields

$$\begin{aligned} \mathcal{L}_v^Q &= \bar{h}_v \left[i \not{D} - \frac{\not{D} \not{D}}{m_Q} - \frac{\not{D} (\not{v} - 1) \not{D}}{4 m_Q} \right] h_v \\ &= \bar{h}_v \left[i v \cdot D - \frac{1}{2 m_Q} \left(D_\mu D^\mu + \frac{1}{4} g_3 \lambda^a \sigma^{\mu\nu} F_{\mu\nu}^a \right) - \frac{(v \cdot D)^2}{2 m_Q} \right] h_v \quad , \end{aligned} \tag{3.14}$$

which is the desired expansion in terms of the heavy quark mass. Because the last term in this expression is second order in $v \cdot D$ and noting that $v \cdot D h_v = 0$ to lowest order, it will not contribute to matrix elements at order $1/m_Q$ and can be dropped. The lagrangian of Eq. (3.14) corresponds to a quark moving at fixed velocity. Antiquark solutions can be constructed with the mass dependence $e^{+i m_Q v \cdot x}$, with the result

$$\mathcal{L}_v^{\bar{Q}} = \bar{k}_v \left[-i v \cdot D - \frac{1}{2 m_Q} \left(D_\mu D^\mu + \frac{1}{4} g_3 \lambda^a \sigma^{\mu\nu} F_{\mu\nu}^a \right) - \frac{(v \cdot D)^2}{2 m_Q} \right] k_v \ , \tag{3.15}$$

where the field k_v satisfies $\Gamma_{v-} k_v = k_v$. It is legitimate to neglect the production of heavy $Q\bar{Q}$ pairs. However, one should superpose the la-

grangians for different velocities in a Lorentz invariant fashion,

$$\mathcal{L} = \int d^4v\ \delta(v_\mu v^\mu - 1)\theta(v_0)\left[\mathcal{L}_v^Q + \mathcal{L}_v^{\bar{Q}}\right] = \int \frac{d^3v}{2v_0}\left[\mathcal{L}_v^Q + \mathcal{L}_v^{\bar{Q}}\right] \quad . \quad (3.16)$$

The nature of the approximation at this stage is more of a classical limit rather than a nonrelativistic limit. To be sure, for any given quark one can work in the quark's rest frame, in which case the quark will be nonrelativistic. However, when external currents act on the fields, as will be considered in Sect. XIV–2, transitions form one frame to another occur for which $\Delta\mathbf{v}$ is *not* small. On the other hand, the result can be said to be classical because quantum corrections have not yet been included and these can renormalize the coefficients in $L_v^{Q\bar{Q}}$. Also, diagrams involving the exchange of hard gluons can produce nonstatic intermediate states. Such corrections can be accounted for in perturbation theory [Wi 91].

XIII-4 Nonconventional hadron states

Many suggestions have been made regarding the possibility of hadronic states beyond those predicted by the simple quark model of $Q\bar{Q}$ and Q^3 configurations. The study of such states is hampered by the fact that we still have very little idea why the quark model works. QCD at low energy is a strongly interacting field theory, and we would expect a very rich and complicated description of hadronic structure. That the result should be describable in terms of a simple $Q\bar{Q}$ and Q^3 picture as even a first approximation remains a mystery. Quark models have been popular because they seem to work phenomenologically, not because they are a controlled approximation to QCD. This weakness becomes all the more evident when one tries to generalize quark model ideas to new areas.

Much of the theoretical work on nonconventional states has involved the concept of a *constituent gluon* G, analogous to a constituent quark Q, and we shall cast our discussion with respect to this degree of freedom.* It is clear that there should be a cost in energy to excite a constituent gluon. The energy should not be extremely large, else it would be difficult to understand the early onset of scaling in deep inelastic scattering. However, it cannot be less than the uncertainty principle bound on a massless particle confined to a radius $R \sim 1$ fm of $E = p \gtrsim \sqrt{3}/R \simeq 342$ MeV (*cf.* Sect. XI–1). Calculations have tended to use an effective gluon 'mass' in the range $0.5 \leq M_G\ (\text{GeV}) \leq 0.6$.

The basic idea of confinement is that only color-singlet states exist as physical hadrons. If we identify those states which are color singlets

* However, it should be understood that such a concept has not been shown to follow rigorously from QCD, nor indeed is a configuration of definite numbers of consitituent gluons a gauge invariant entity (*cf.* Sect. X–2).

and which contain few quark or gluon quanta, we can easily find other possible configurations besides $Q\bar{Q}$ and Q^3. Some of the more well-known examples are

1) Gluonia (or glueballs) – quarkless G^2 or G^3 states, which we shall discuss in more detail below,
2) Hybrids – color-singlet mixtures of constituent quarks and gluons like $Q\bar{Q}G$ mesons or Q^3G baryons,
3) Dibaryons – six-quark configurations in which the quarks have *similar* spatial wavefunctions rather than two separate three-quark clusters,
4) Meson molecules – loosely bound deuteron-like composites of mesons.

A convenient framework for describing the quantum numbers of possible hadronic states is obtained by considering gauge-invariant, color-singlet operators of low dimension [JaJR 86], as was discussed in Sect. XI–1. Table XIII–4 lists all such operators up to dimension five which can be constructed from quark fields, the QCD covariant derivative, and the gluon field strength, denoted respectively by q, $\mathcal{D}$, and F. Also appearing in Table XIII–4 is the collection of J^{PC} quantum numbers associated with each such operator. Particular spin-parity values are obtained from these operators by choosing indices in appropriate combinations.

Gluonia

The existence of a gluon degree of freedom in hadrons is beyond dispute, with evidence from deep inelastic lepton scattering and jet structure in hadron-hadron collisions. However, trying to predict the properties of a new class of hadrons whose primary ingredient is gluonic is nontrivial. Hypothetically, if quarks could be removed from QCD the resulting hadron spectrum would consist only of *gluonia* (or 'glueballs').

Gluonic configurations should be signaled by the existence of extra states beyond the expected nonets of $Q\bar{Q}$ hadrons. However, mixing with $Q\bar{Q}$ hadrons is generally possible (*cf.* Sect. X–2). Although predicted by

Table XIII–4. Gauge-invariant color-singlet interpolating fields.

Operator	Dimension	J^{PC}
$\bar{q}\Gamma q$	3	$0^{-+}, 1^{--}, 0^{++}, 1^{+-}, 1^{++}$
$\bar{q}\Gamma\mathcal{D}q$	4	$2^{++}, 2^{-\pm}$
FF	4	$0^{++}, 2^{++}, 0^{-+}, 2^{-+}$
$\bar{q}\Gamma qF$	5	$0^{\pm+}, 0^{\pm-}, 1^{\pm+}, 1^{\pm-}, 2^{\pm+}, 2^{\pm}$
$F\mathcal{D}F$	5	$1^{++}, 3^{++}$

the $1/N_c$ expansion to be suppressed, such mixing effects serve to cloud the interpretation of data vis-à-vis gluonium states. Referring to the interpolating fields mentioned above, we see that for gluons the gauge-invariant combinations

$$F^a_{\mu\nu}F^{\mu\nu}_a\,, \qquad F^a_{\mu\lambda}F^{\lambda}_{a\nu}\,, \qquad F^a_{\mu\nu}\tilde{F}^{\mu\nu}_a\,, \qquad F^a_{\mu\lambda}\tilde{F}^{\lambda}_{a\nu} \tag{4.1}$$

can be formed out of *two* factors of a gluon field-strength tensor $F^a_{\mu\nu}$ or its dual $\tilde{F}^{\mu\nu}_a$. The spin, parity, and charge conjugation carried by these these operators are respectively $J^{PC} = 0^{++}$, 2^{++}, 0^{-+}, 2^{-+}, and are thus the quantum numbers expected for the lightest glueballs,* *i.e.* such operators acting on the vacuum state produce states with these quantum numbers. Although there is no *a priori* guarantee that one obtains a single particle state (*e.g.* a 2^{++} operator could in principle create two 0^{++} glueballs in a D-wave), the simplicity of the operators leads one to suspect that this will be the case. There is one, somewhat controversial, construct missing from the above list. Two massive spin-one particles in an S-wave can have $J^{PC} = 1^{-+}$ as well as $J^{PC} = 0^{++}, 2^{++}$, and some models predict such a gluonium state. However, a 1^{-+} combination of two massless on-shell vector particles is forbidden by a combination of gauge invariance plus rotational symmetry [Ya 50]. The lack of a 1^{-+} gauge-invariant, two-field operator is an indication of this.

Aside from a list of quantum numbers and some guidance as to relative mass values, theory does not provide a very clear profile of gluonium phenomenology. Lattice-gauge methods offer the most hope for future progress. At present, they predict in a quarkless version of QCD that the lightest glueball will be a 0^{++} state of mass 1.2 ± 0.3 GeV and that the 2^{++} glueball is 1.5 ± 0.1 times heavier [BaK 89].

Gluonium states would be classified as flavor-$SU(3)$ singlets. One process expected to lead to direct production of glueballs is the radiative decay of J/ψ, which takes place in QCD through the annihilation process $c\bar{c} \to \gamma GG$ (as in Fig. XIII–4(c)). The two gluons emerge in a color singlet configuration, and by varying the energy of the final-state photon, all masses between $m = 0$ and $m \simeq M_{J/\psi}$ can be probed. A glueball should thus be revealed as a resonance M in the decay $J/\psi \to \gamma M$. Of course, $Q\bar{Q}$ states can be produced as well. In order to distinguish gluonia from such neutral quark states, a measure S_M, whimsically called the 'stickiness' of meson M, has been introduced [Ch 84],

$$S_M \equiv \frac{\Gamma_{J/\psi\to\gamma M}}{\Gamma_{\gamma\gamma\to M}} \times \frac{\text{p.s. } [\gamma\gamma \to M]}{\text{p.s. } [J/\psi \to \gamma M]} \tag{4.2}$$

---

* Gluonic operators with *three* field-strength tensors produce states with $J^{PC} = 0^{\pm+}$, $1^{\pm+}$, $2^{\pm+}$, $1^{\pm+}$, $2^{\pm-}$, $3^{\pm-}$. Because of the extra gluon field, one expects these states to be somewhat heavier.

where 'p.s.' stands for the available phase space. A glueball would be expected to couple strongly to GG but not to $\gamma\gamma$, and thus to have a high relative value of stickiness compared to a $Q\bar{Q}$ composite.

Let us consider two states, among others under active investigation, which are strongly produced in $J/\psi \to \gamma M$ and have provoked much attention as possible anomalous states. These are the $f_2(1720)$ and $\eta(1440)$, also called $\theta(1720)$ and $\iota(1440)$ respectively. Evidence to date suggests that $f_2(1720)$ (*i.e.* θ) has the properties of a non-$Q\bar{Q}$ system. It is a resonance seen primarily in $J/\psi \to \gamma f_2(1720) \to \gamma K\bar{K}$ and has been assigned the quantum numbers $J^{PC} = 2^{++}$. The $\pi\pi$ and $\eta\eta$ decay modes have also been observed, with the quoted branching ratios

$$\mathrm{Br}_{\theta\to K\bar{K}} : \mathrm{Br}_{\theta\to\eta\eta} : \mathrm{Br}_{\theta\to\pi\pi} \simeq 1.00 : 0.47 : 0.10 \quad . \tag{4.3}$$

The dominance of $K\bar{K}$ is even more striking when one notes that D-wave phase space favors the $\pi\pi$ mode by a factor $\simeq 2.6$.

The $Q\bar{Q}$ 2^{++} ground states are $f_2(1270)$ and $f_2'(1525)$, with dominant components $(u\bar{u}+d\bar{d})/\sqrt{2}$ and $s\bar{s}$ as deduced from their decays. If θ were a $Q\bar{Q}$ state, it would be a radial excitation of the f_2 and f_2'. However, the θ is too close in mass to the $f_2'(1525)$ to be its radial excitation, and the θ decay pattern requires its interpretation as largely $s\bar{s}$, so that it cannot be the radial excitation of the $f_2(1270)$. Besides, there is some experimental evidence identifying the radial excitation of $f_2(1270)$ at 1800 MeV. The θ has not been seen in other hadronic reactions where $f_2(1270)$ and $f_2'(1525)$ stand out strongly, and its stickiness is remarkable,

$$S_f : S_{f'} : S_\theta = 1 : 3 : > 20 \quad . \tag{4.4}$$

Even if one accepts that θ is not a $Q\bar{Q}$ hadron, a firm identification of its primary content is still difficult. The high stickiness and lack of any known multiplet partners favor a glueball interpretation, but its decays do not seem $SU(3)$ symmetric. Additional knowledge of the $J^{PC} = 2^{++}$ spectrum and further experimentation will be required to clarify this issue. Indeed, a new analysis [Du 92] reports evidence that $J^{PC} = 0^{++}$ for the θ. If this turns out to be correct, the difficulties of accommodating the θ as a $Q\bar{Q}$ state may not be as severe.

The other interesting glueball candidate is the iota, $\iota(1440)$. It is the $J^{PC} = 0^{-+}$ state with the largest branching fraction in J/ψ radiative decays, but appears as a rather obscure resonance in hadronic reactions. In comparison with $\eta(549)$ and $\eta'(960)$, it has stickiness ratios

$$S_\eta : S_{\eta'} : S_\iota = 1 : 4 : > 45 \quad , \tag{4.5}$$

which would favor a glueball interpretation. However, the situation regarding hadronic experiments which probe the $J^{PC} = 0^{-+}$ spectrum in the range 1.0–1.7 GeV is presently so confused that even $Q\bar{Q}$ states cannot be identified with any certainty. As with all gluonium states, the

situation will continue to be distressingly vague without a good deal of additional experimental and phenomenological guidance.

Additional nonconventional states

There is a widespread belief that gluonium states *must* appear in the spectrum of the QCD hamiltonian. For other kinds of nonconventional configurations, it is far more difficult to reach a meaningful consensus, although experimental efforts to detect such states continue. Let us briefly review several such possibilities.

(i) *Hybrids*: From Table XIII–4, we see that among the $\bar{Q}QG$ meson hybrids is one with the quantum numbers $J^{PC} = 1^{-+}$. This would-be hadron is of particular interest because comparison with Table XI–3 reveals that it cannot be a $\bar{Q}Q$ configuration. Model calculations suggest that the lightest such state should be isovector, with mass in the range 1.5–2.0 GeV, and that such states may largely decouple from $L = 0$ $\bar{Q}Q$ meson final states. A study of Q^3G baryon hybrids reveals that *none* of the states is exotic in the sense of lying outside the usual Q^3 spectrum [GoHK 83].

(ii) *Dibaryons*: The most remarkable aspect learned yet about the dibaryon states is how much six-quark configurations are restricted by Fermi-Dirac statistics. Table XIII–5 lists the possible six-quark $SU(3)$ multiplets along with their spin values [Ja 77]. Of this collection of states, most attention has been given to the spinless $SU(3)$-singlet state, called the *H-dibaryon.* This particle, which has strangeness $S = -2$ and isospin $I = 0$, is predicted to be the lightest dibaryon, and to be unstable to weak decay. Although evidence for the H is limited to observation of a neutral object decaying to $p + \Sigma^-$ [ShSKM 90], experimental searches continue.

(iii) *Hadronic molecules*: Together with the glueball candidates discussed earlier, another possible interpretation of observed particles as

Table XIII–5. Spectroscopy of six-quark configurations.

$SU(6)$ of color-spin	$SU(3)$ of flavor	Spin
490	1	0
896	8	1,2
280	10	1
175	10*	1,3
189	27	0,2
35	35	1
1	28	0

nonconventional hadrons occurs with the isovector $a_0(980)$ and isoscalar $f_0(975)$ mesons. Nominally, these particles have the quantum numbers of the $L = 1$ sector of the $Q\bar{Q}$ model, and their near equality in mass suggests an internal composition similar to that of the $\rho(770)$ and $\omega(783)$, *i.e.* orthogonal configurations of nonstrange quark-antiquark pairs. However, among properties which argue against this are their relatively strong coupling to modes which contain strange quarks, their narrower-than-expected widths, and their $\gamma\gamma$ couplings. The proximity of the $K\bar{K}$ threshold and the importance of the $K\bar{K}$ modes has motivated their interpretation as $K\bar{K}$ molecules [WiI 83]. Unfortunately, interpretation of scattering data near the 1 GeV region is confused, with even the very number of isocalar states in question [AuMP 87].

Problems

1) **Power law potential in quarkonium**
Consider an interquark potential of the form $V(r) = cr^d$.
   a) Use the virial theorem to determine $\langle T\rangle/\langle V\rangle$ for the ground state.
   b) Given the form $E_{2S} - E_{1S} = f(d)M^{-d/(2+d)}$, where M is the reduced mass, determine d from the observed mass differences in the $c\bar{c}$ and $b\bar{b}$ systems, using Eq. (3.1) to supply heavy-quark mass values.
   c) Assuming this model is used to fit the spin-averaged ground state $c\bar{c}$ and $b\bar{b}$ mass values, determine $\mathbf{v}^2/c^2$ for each system.
2) **Quarkonium annihilation from the $^1S_0$ state**
Modify Eq. (1.20) to obtain the leading-order contributions appearing in Eq. (1.21).
3) **Spin-dependence and light P-wave mesons**
   a) Numerically determine the quantities $\bar{m}, m_{\mathrm{s-o}}, m_{\mathrm{ten}}$ of Eq. (1.10) using $n = 1$ Υ P-wave mass values.
   b) Repeat this evaluation for light P-wave mesons, but include a $^1P_1$ state in your analysis. Thus, you must generalize Eq. (1.10) to include a spin-spin contribution m_{ss}. Choose mass values according to the assignments

$$^1P_1 \to K_1(1400)\ , \qquad ^3P_J \to \begin{cases} K_2(1430) & (^3P_2) \\ K_1(1270) & (^3P_1) \\ K_0(1430) & (^3P_0)\ . \end{cases}$$

   Comparison of the results with the QCD Breit-Fermi interaction of Eq. (2.10) reveals the real world to have a smaller spin-orbit effect than is (at least naively) anticipated from this model.

4) **Mass relations involving heavy quarks**
   a) Repeat the analysis of Eq. (3.1) but using the masses of the charmed/strange mesons D_s, D_s^* instead. Infer a value for $\hat{M}/M_c$ by referring to the result obtained in Eq. (2.17). Compare with the determination of Eq. (3.1).
   b) Extend the procedure of Eqs. (2.20-2.25) to isospin-violating mass differences of c-flavored and b-flavored hadrons.